



HAL
open science

Experimental Study on Oscillatory Couette-Taylor Flows Behaviour

Emna Berrich, Fethi Aloui, Jack Legrand

► **To cite this version:**

Emna Berrich, Fethi Aloui, Jack Legrand. Experimental Study on Oscillatory Couette-Taylor Flows Behaviour. ASME 2013 Fluids Engineering Division Summer Meeting, Jul 2013, Incline Village, United States. 10.1115/FEDSM2013-16308 . hal-01206891

HAL Id: hal-01206891

<https://imt-atlantique.hal.science/hal-01206891>

Submitted on 14 Jun 2021

HAL is a multi-disciplinary open access archive for the deposit and dissemination of scientific research documents, whether they are published or not. The documents may come from teaching and research institutions in France or abroad, or from public or private research centers.

L'archive ouverte pluridisciplinaire **HAL**, est destinée au dépôt et à la diffusion de documents scientifiques de niveau recherche, publiés ou non, émanant des établissements d'enseignement et de recherche français ou étrangers, des laboratoires publics ou privés.



Distributed under a Creative Commons Attribution 4.0 International License

EXPERIMENTAL STUDY ON OSCILLATORY COUETTE - TAYLOR FLOWS BEHAVIOUR

Emna BERRICH¹

Emna.berrich@mines-nantes.fr

*** Fethi ALOUI**²

* Corresponding author:
Fethi.aloui@univ-valenciennes.fr

Jack LEGRAND³

Jack.Legrand@univ-nantes.fr

¹ LUNAM Université, Université de Nantes,
CNRS, GEPEA, UMR6144, École des Mines de Nantes,
4 rue Alfred KASTLER - BP20722 44307 Nantes Cedex 03 - France

² Université de Valenciennes et du Hainaut-Cambrésis,
Laboratoire TEMPO EA 4542, DF2T, Campus Mont Houy, F-59313 Valenciennes Cedex 9 - France

³ LUNAM Université, Université de Nantes, CNRS, GEPEA, UMR6144, CRTT,
37 Boulevard de l'Université BP 406, 44602 Saint-Nazaire Cedex - France

ABSTRACT

In the simplest and original case of study of the Taylor–Couette TC problems, the fluid is contained between a fixed outer cylinder and a concentric inner cylinder which rotates at constant angular velocity. Much of the works done has been concerned on steady rotating cylinder(s) i.e. rotating cylinders with constant velocity and the various transitions that take place as the cylinder(s) velocity (ies) is (are) steadily increased. On this work, we concentrated our attention in the case in which the inner cylinder velocity is not constant, but oscillates harmonically (in time) clockwise and counter-clockwise while the outer cylinder is maintained fixed. Our aim is to attempt to answer the question if the modulation makes the flow more or less stable with respect to the vortices apparition than in the steady case. If the modulation amplitude is large enough to destabilise the circular Couette flow, two classes of

axisymmetric Taylor vortex flow are possible: reversing Taylor Vortex Flow (RTVF) and Non-Reversing Taylor Vortex Flow (NRTVF) (Youd et al., 2003; Lopez and Marques, 2002). Our work presents an experimental investigation of the effect of oscillatory Couette-Taylor flow, i.e. both the oscillation frequency and amplitude on the apparition of RTVF and NRTVF by analysing the instantaneous and local mass transfer and wall shear rates evolutions, i.e. the impact of vortices at wall. The vortices may manifest themselves by the presence of time-oscillations of mass transfer and wall shear rates, this generally corresponds to an instability apparition even for steady rotating cylinder. On laminar CT flow, the time-evolution of wall shear rate is linear. It may be presented as a linear function of the angular velocity, i.e. the evolution is steady even if the angular velocity is not steady. At a “critical” frequency and amplitude, the laminar CT flow is disturbed and Taylor

vortices appear. Comparing to a steady velocity case, oscillatory flow accelerate the instability apparition, i.e. the critical Taylor number corresponds to the transition is smaller than that of the steady case. For high oscillation amplitudes of the inner cylinder rotation, the mass transfer time-evolution has a sinusoidal evolution with non equal oscillation amplitudes. If the oscillation amplitude is large enough, it can destabilize the laminar Couette flow, Taylor vortices appears. The vortices direction can be deduced from the sign of the instantaneous wall shear rate time evolution.

Keywords: *Oscillatory Couette-Taylor flows; Reversing and Non-Reversing Taylor Vortex Flow RTVF & NRTVF; Mass Transfer rate; Wall Shear Stress; Inverse method.*

1. INTRODUCTION

Taylor-Couette flows are frequently re-encountered on engineering processes (such on rotor-stator systems) and medical applications. It is widely used for the depleted uranium enrichment, as a membrane or filter, on bioreactors and for blood detoxification. Most of the studies were interested to the Couette-Taylor simple case where the fluid is contained between a fixed outer cylinder and a concentric inner cylinder which rotates at constant angular velocity. Much of the works done has been concerned on steady rotating cylinder(s) i.e. rotating cylinders with constant velocity and the various transitions that take place as the cylinder(s) velocity (ies) is (are) steadily increased. On this work, we concentrated our attention in the case in which the inner cylinder velocity is not constant, but oscillates harmonically (in time) clockwise and counter-clockwise while the outer cylinder is maintained fixed. Our aim is to attempt to answer the question if the modulation makes the flow more or less stable with respect to the vortices apparition than in the steady case.

If the modulation amplitude is large enough to destabilise the circular Couette flow, two classes of axisymmetric Taylor vortex flow are possible: Reversing Taylor Vortex Flow (RTVF) and Non-Reversing Taylor Vortex Flow (NRTVF). For Reversing Flow, the inner cylinder is rotating anti-clockwise for the first part of the cycle; the vortices respond by rotating in the same direction of the cylinder motion. For the second part of the cycle, the inner cylinder rotates in the opposite direction, the vortices respond by changing their rotation direction. For Non-Reversing Flow, the inner cylinder is rotating anti-clockwise and the vortices rotate in the same direction of the cylinder motion. However, when the inner cylinder reverses its rotation direction, the vortices continue to rotate in the same direction as in the first half-cycle. Youd et al., (2003) [1] studied numerically the two flow types. They used a combination of second-order accurate Crank-Nicolson and Adams-Bashforth methods. The velocity components are represented by potentials which were expanded spectrally over Fourier modes in the azimuthal and axial directions and over Chebyshev polynomials in the radial direction. More details on numerical code are

available on Willis & Barenghi [2]. Their code has been tested in the linear and nonlinear axisymmetric regime by using Barenghi [3] and Jones [4] results. Youd et al. [1] demonstrated that for relatively high oscillation frequencies, the Taylor vortices direction does not change every half-cycle, i.e. presence of NRTVF. Youd et al., [5] proved that, for Couette-Taylor system characterized by a radial ratio $\eta = R_{\text{int}}/R_{\text{out}} = 0.75$, there was a transition to a new kind of axisymmetric time-modulated flow, i.e. the Non-Reversing Taylor Vortex Flow (NRTVF) in which the rotation direction of the Taylor vortices is independent on the inner cylinder rotation direction. They illustrated that if the oscillation amplitude is large enough, it is possible that the resulting time-dependent Taylor vortex rotates in a direction which does not depend on the direction of the azimuthal motion which drives it. The transition to this “non-reversing” Taylor vortex flow is examined as a function of oscillation frequency and radial ratio η . Taylor vortex pairs always rotate in the same direction, despite the inner cylinder driving the flow in the opposite direction. NRTVF takes place at sufficiently high modulation frequencies for which there is not enough time for the toroidal motion to vanish to sufficiently small values, i.e. these frequencies are small enough so that $\delta_s = (2\nu/\omega)^{1/2}$, where ν is the kinematic viscosity and ω the oscillation frequency, is the thickness of the Stokes layer generated when the oscillating boundary induces a damped viscous wave which penetrates into the fluid, is comparable to the length scale $\delta = R_2 - R_1$. NRTVF can be caused by linear instability [6] or finite-amplitude effects [1]. NRTVF may be affected by the weak Ekman circulation (absent in the calculation of Youd et al., [1]) which is necessarily induced by the fixed top and bottom ends of the Taylor-Couette System. Carmi and Tustaniwskyj [7] numerically studied oscillatory Couette flow. They did not detect the existence of NRTVF. Their approach was based on studying the effects of infinitesimal perturbations over a cycle, i.e. the Floquet theory. The stability of the basic state can be determined by Floquet analysis, where the Navier-Stokes equations are linearized about the basic state, the linear system with a complete basis for general perturbations can be evolved for a period. More details about the theory are available on [5, 6]. It is possible that NRTVF is due to finite-amplitude effects, whereas in RTVF, the radial velocity becomes negative for part of the cycle, NRTVF decays only to a certain order of magnitude level, at the end of a cycle, never becoming infinitesimal. However, non-reversing solutions have been found by Lopez & Marques [7] using Floquet analysis for oscillation of the outer cylinder, so NRTVF could be due to a linear instability too. Our work presents an experimental investigation of the effect of oscillatory Couette-Taylor flow, i.e. both the oscillation frequency and amplitude on the apparition of RTVF and NRTVF by analysing the instantaneous and local mass transfer and wall shear rate evolutions, i.e. the impact of vortices at wall.

NOMENCLATURE

| | |
|----------------------|---|
| a : | : Inner cylinder radius (m) |
| A : | : Surface of the probe (m^2) |
| C : | : Concentration (mol/m^3) |
| D : | : Coefficient of diffusion ($m^2.s^{-1}$) |
| F : | : Frequency of oscillation (Hz) |
| H : | : Height of the CTS |
| I : | : Current (A) |
| l : | : Probe length |
| Pe : | : Péclet number |
| R : | : Radius (m) |
| Re : | : Reynolds number |
| S : | : Wall shear stress (s^{-1}) |
| Sh : | : Sherwood number |
| t : | : Time (s) |
| Ta : | : Taylor number |
| u : | : Velocity ($m.s^{-1}$) |
| x, z : | : Coordinates (m) |
| Greek symbols | |
| β : | : Amplitude of the oscillation |
| Ω : | : Angular velocity of the rotating plate ($rad.s^{-1}$) |
| ν : | : Kinetic viscosity ($m^2.s^{-1}$) |
| δ : | : $\delta = R_2 - R_1$ (m) |
| η : | : Radial ratio |
| Γ : | : Aspect ratio |
| Superscripts | |
| * | Dimensionless |
| - | Temporal average |
| Subscripts | |
| a | : inertia effect |
| ax | : axial |
| c | : critical |
| $cent$ | : centrifugal force |
| i | : inner |
| $q.l.$ | : quasi-linear |
| Lev | : Lévêque approach |
| Sob | : Sobollik et al. approach |

2. EXPERIMENTAL INSTALLATION

The experimental installation is composed of an inner cylinder with a radius $R_1=97\pm 0.2$ mm and an outer cylinder with a radius $R_2=100\pm 0.2$ mm. The corresponding radius ratio is $\eta=0.97$ and the aspect ratio is $\Gamma=150$. The whole apparatus is made in Plexiglas (figure 1a). The inner cylinder was driven by a α -Step motor (marketed by the Omeron company). The electrical motor imposed to the mobile inner cylinder a maximum speed of 120 rpm. It was supplied by a signal generator. The revolutions were controlled by a speed controller. The engine assures to impose sinusoidal motion to the inner cylinder.

Polarography technique, known as the limiting diffusion current method, has been used. This requires the use of Electro-Diffusion ED probe which allows the determination of the local mass transfer rate from Limiting Diffusion current measurement delivered by the probe while it is polarized by a polarization voltage. In addition, a series of platinum probes have been mounted flush to the inner surface of the outer cylinder of the

Couette Taylor System. ED results are presented for the probe G (see Figure 1a and 1b), for different oscillation amplitudes as well as for high and low oscillation frequencies. The wall shear stress has been determined using different solutions mostly used in polarography, such as the Lévêque solution [8] and the quasi-steady solution of Sobollik [9] and the inverse method [10].

3. POLAROGRAPHY TECHNIQUE

In our tests, we have used a ferri-ferrocyanure of potassium as electrochemical solution with a concentration of $25 mol/m^3$, with a dispersion of 2.5% of Kalliroscope particles to visualize the flow, an excess of the sulfate of potassium K_2SO_4 ($130 mol/m^3$) as supporting electrolyte and 40% of Glycerin to relay the instability apparition (viscosity effect).

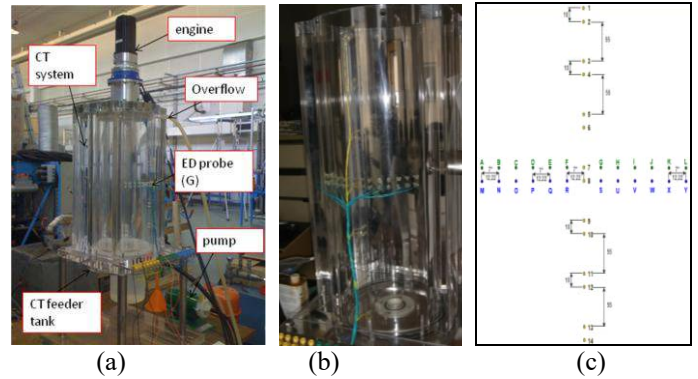


Figure 1. (a) Experimental installation; b) Electrochemical probes disposition on the inner wall of the outer cylinder; b) Notations and coordinates of the electrochemical probes used

4. STEADY TAYLOR VORTEX FLOW CHARACTERIZATION

To attempt to answer the question if the modulation makes the flow more or less stable with respect to the vortices apparition than in the steady case, we begin by characterizing the flow for the case where the inner cylinder rotates at constant angular velocity i.e. on steady case.

The Taylor number is generally used to characterize modes transition. It describes the competition between the viscous dissipation and the centrifugal force. It is defined as:

$$Ta = \frac{\tau_v}{\tau_{cent}} = \frac{\Omega R_{int} \delta}{\nu} \sqrt{\frac{\delta}{R_{int}}} = Re_i \sqrt{\frac{\delta}{R_{int}}} \quad (1)$$

where the Reynolds number describes the competition between the viscous dissipation and the inertia effect:

$$Re = \frac{\tau_v}{\tau_a} = \frac{\Omega R \delta}{\nu} \quad (2)$$

The time-evolution of the Taylor number is presented on figure 2. It shows that the Taylor number is constant and that the average Taylor number is equal to 8 ± 0.4 . For this Taylor number, we studied the time-evolution of the mass transfer and the wall shear rates. This allows flow instability detection because the vortices manifest themselves by the apparition of

variations on mass transfer and wall shear rates. The dimensionless mass transfer rate is almost constant (figure 3). The average value is equal to 1 ± 0.02 . The flow is thus steady. It corresponds to Couette flow. The time-evolution of dimensionless wall shear rate for $Ta=8$ is presented on figure 4. The dimensionless wall shear rate remains constant. The average value is equal to 1 ± 0.05 . The flow is thus stable and no vortices appear. To conclude, on laminar CT flow, the time-evolution of wall shear rate is linear. It may be presented as a linear function of the angular velocity.

For the same average inner cylinder velocity, we studied the effect of oscillations on flow for different amplitude and frequencies modulations.

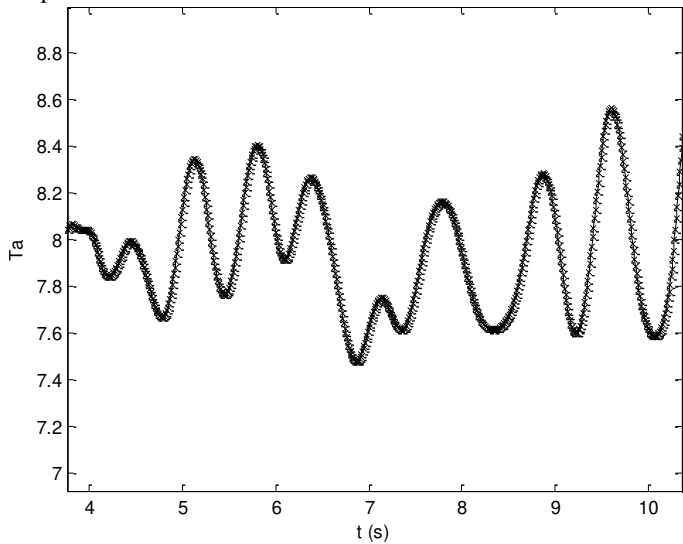


Figure 2. Evolution of the Taylor number for steady flow case

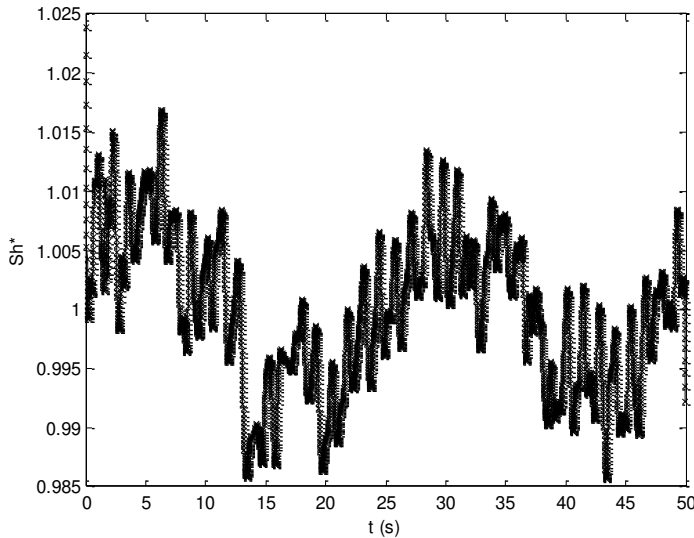


Figure 3. Evolution of dimensionless mass-transfer rate for $Ta_m=8$

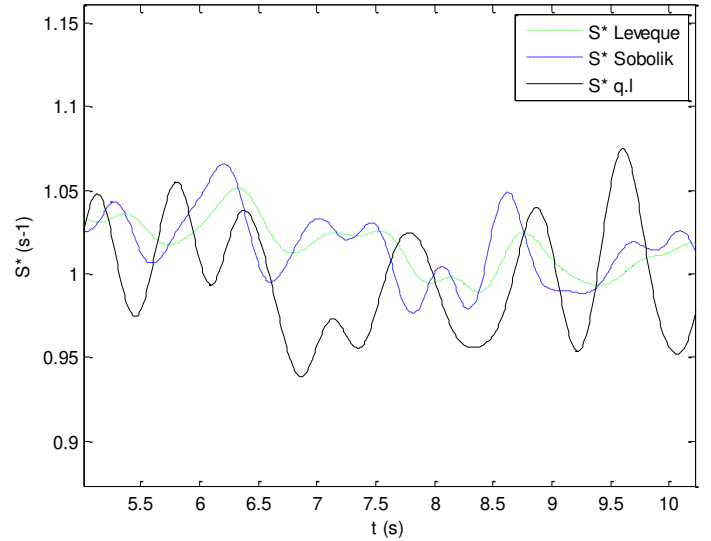


Figure 4. Evolution of dimensionless wall shear stress for $Ta_m=8$

5. MODULATION AMPLITUDE EFFECT ON RTVF AND NRTVF

5.1. Protocols and Taylor number evolutions

As the Reversing Taylor Vortex Flow RTVF and the Non Reversing Taylor Vortex Flow NRTVF strongly depend on the inner cylinder rotation direction, we studied three principle protocols:

- CASE A: The first one corresponds to non-stop advancing inner cylinder i.e. the inner cylinder always advances while oscillating. In this case, the Taylor number remains strictly positive and the modulation amplitude β is strictly lesser than the unit.
- CASE B: The second protocol corresponds to advancing – stopped inner cylinder. The Taylor number time-evolution presents then a zero Taylor number when the inner cylinder is stopped and strictly positive values when it advances. In this case, the modulation amplitude β should be equals to the unit.
- CASE C: The third case corresponds to the case where the inner cylinder advance then moves back then advances again. The Taylor numbers presents thus positives values for a half cycle and negative values for the other half cycle. The modulation amplitude β should be bigger than the unit. We studied several cases depending on modulation amplitudes (bigger than the unit).

The time-evolutions of the Taylor number are shown respectively on figure 5 (case A), figure 6 (case B), and figures 7 and 8 (cases C) respectively for modulation amplitudes $\beta = 4.96$ (case C.1) and $\beta = 9.73$ (case C.2).

As we can see, for the different oscillatory cases, the time evolution of the Taylor number presents a sinusoidal evolution characterizing the oscillatory flow presence. The average Taylor number is equal to 8 which correspond to Taylor number for the steady case studied on the first section. For example, the Taylor number varies between 12 and 4 (case A). It oscillates between 0 and 16 (case B) and between -31 and 47 (case C.1). So, the average Taylor number is equals to 8 which correspond to Taylor number for the steady laminar Couette flow case studied on the first section. As we have proved that for Taylor number equal to 8, the flow corresponds to laminar Couette Flow. The question now is if the oscillation disturbs the flow enough and accelerates the transition apparition. We propose an answer by analyzing the mass transfer and the wall shear rates.

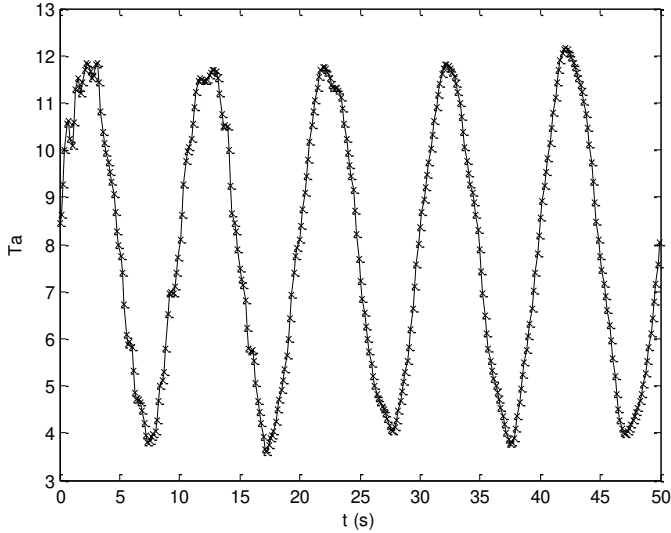


Figure 5. Evolution of the Taylor number for $F=100$ mHz and $\beta=0.53$ (case A)

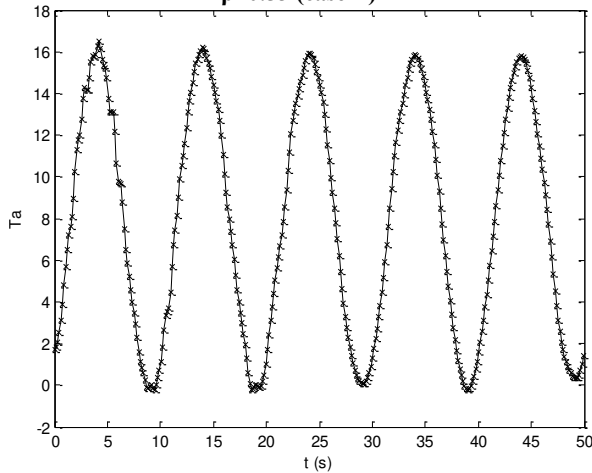


Figure 6. Evolution of the Taylor number for $Ta_m=8$, $F=100$ mHz and $\beta=1.08$ (case B)

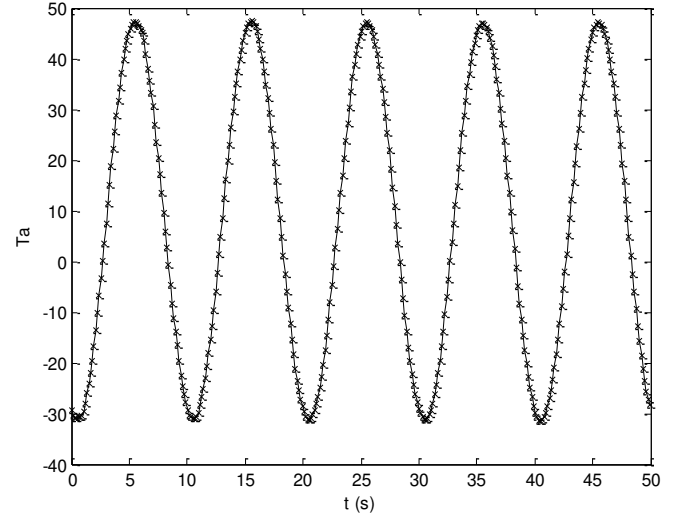


Figure 7. Evolution of the Taylor number for $Ta_m=8$, $F=100$ mHz and $\beta=4.96$ (case C.1)

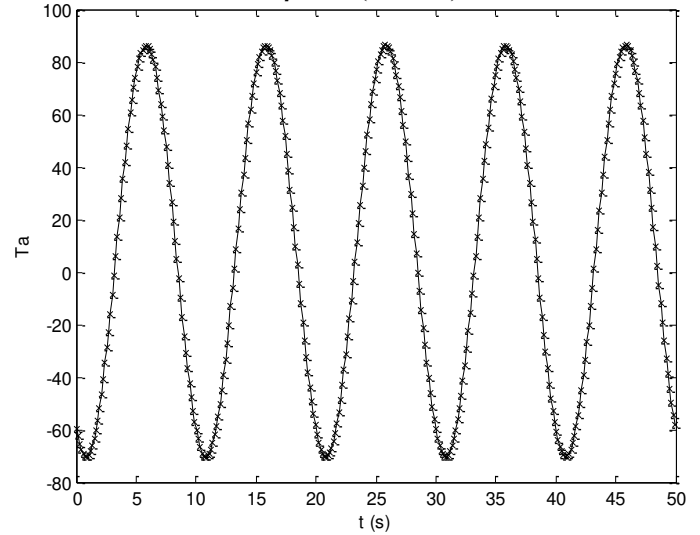


Figure 8. Evolution of the Taylor number for $Ta_m=8$, $F=100$ mHz and $\beta=9.73$ (case C.2)

5.2. Mass transfer rates analysis

Mass transfer rates time-evolution i.e. the Sherwood number for the different oscillatory flow are presented respectively on figure 9 (case A), figure 10 (case B), and figure 11 and 12 (cases C) respectively for modulation amplitudes $\beta = 4.96$ (case C.1) and $\beta = 9.73$ (case C.2).

The Sherwood number is defined by:

$$Sh = \frac{il}{nFC_0AD} \quad (3)$$

Where i is the Limiting Diffusion current delivered by the Electro-Diffusion ED probe, l the probe length, n the ions number, F the Faraday number, C_0 the initial concentration, A the probe area and D the coefficient of Diffusion.

The instantaneous and local mass transfer rates evolutions demonstrate the apparition and development of Taylor vortices

which manifest themselves by the presence of oscillations having constant amplitudes for $\beta = 0.53$ (case A) and $\beta = 1.08$; and non constant amplitudes for sufficiently high amplitudes (cases C); despite that the mean Taylor number corresponds to a steady case i.e. Couette flow. So, we can deduce that oscillations accelerate the transition apparition and thus the critical Taylor number corresponding to the transition from laminar Couette flow to Wavy Vortex flow is lesser than that of the steady case. For high modulation amplitudes, the mass transfer time-evolution has a sinusoidal evolution with non equal oscillation amplitudes. If the oscillation amplitude is large enough, it can destabilize the laminar Couette flow, Taylor vortices appears. The mass transfer rate remains always positive in all the studied cases. The vortices direction can be deduced from the sign of the instantaneous wall shear rate.

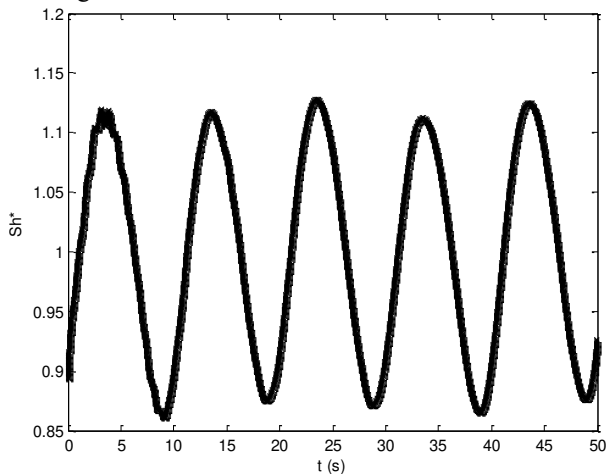


Figure 9. Evolution of dimensionless mass-transfer rate for $Ta_m=8$, $F=100$ mHz and $\beta=0.53$

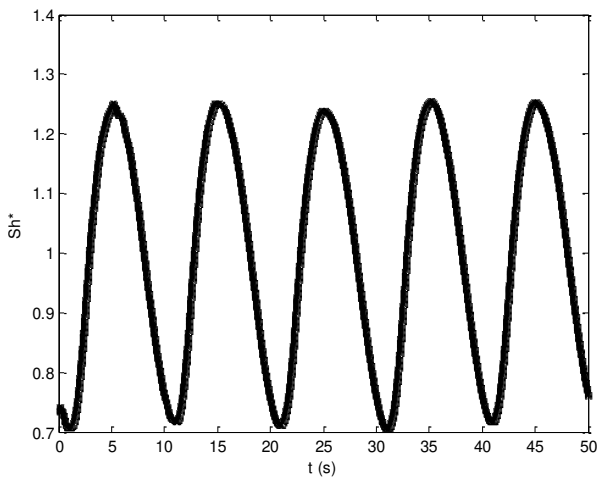


Figure 10. Evolution of dimensionless mass-transfer rate for $Ta_m=8$, $F=100$ mHz and $\beta=1.08$

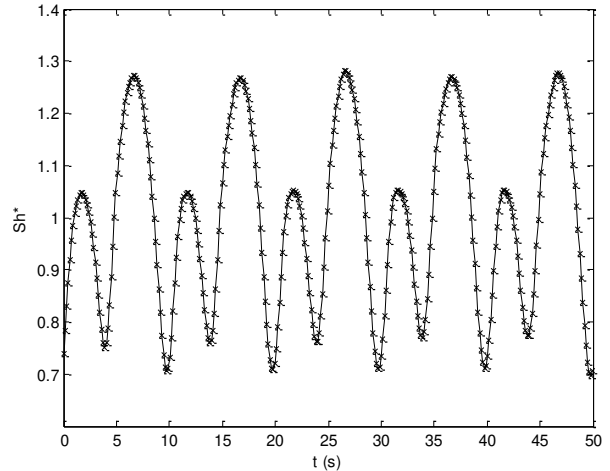


Figure 11. Evolution of dimensionless mass-transfer rate for $Ta_m=8$, $F=100$ mHz and $\beta=4.96$

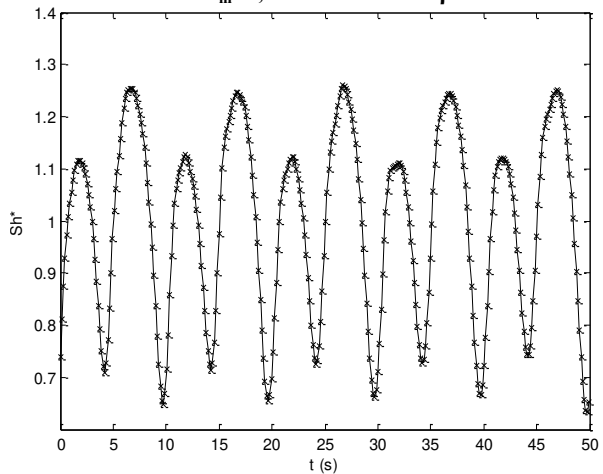


Figure 12. Evolution of dimensionless mass-transfer rate for $Ta_m=8$, $F=100$ mHz et $\beta=9.73$

5.3. Wall shear rates analysis

Basing on mass transfer evolutions, we have found that, if the oscillation amplitude is large enough, laminar Couette flow can be destabilized, Taylor vortices appears. The vortices direction can be deduced from the sign of the instantaneous wall shear rate time evolution. Even if the limiting diffusion current sign is positive thus the mass transfer sign still positive, the sign of the wall shear rate can be negative which may corresponds to RTVF.

In all the oscillatory cases studied, the average Taylor number is equal to 8 which correspond to Taylor number for the steady case corresponding to laminar Couette flow. The impact of vortices, if they appear, on the inner wall of the outer cylinder can be studied via the local and instantaneous mass transfer rate and wall shear rate. The wall shear rate was determined using three approaches. The first one is the “Lévêque solution” [8] which relate the local and instantaneous mass transfer to the local and instantaneous wall shear rate:

$$S_{Lev} = \frac{D}{l^2} \left(\frac{Sh(t)}{0.807} \right)^3 \quad (4)$$

This method is valid on steady regime, for high Péclet numbers and when the axial diffusion can be neglected. The second approach is the Sobolik et al. [9] method which is a correction of the Lévêque [8] solution:

$$S_{Sob}(t) = S_q(t) + \frac{2}{3} \theta(t) \left(\frac{\partial S_q(t)}{\partial t} \right) \quad (5)$$

where:

$$S_q = S_{Lev} = \frac{D}{l^2} \left(\frac{Sh(t)}{0.807} \right)^3 \quad (6)$$

and:

$$\theta(t) = 0.486 l^{\frac{2}{3}} D^{-\frac{1}{3}} S_q(t)^{-\frac{2}{3}} \quad (7)$$

Sobolik et al. [9] added a term obtained from the unsteady response of the ED probe multiplied by the time derivative of the mass transfer rate. Rehimy *et al.* [10] applied the inverse method using simulated data to determine wall shear rate. They tested the sequential estimation for a known wall shear rate of the form:

$$S^*(t) = 1 + \beta \cos(2\pi f t^* + \varphi) \quad (8)$$

The instantaneous Sherwood number can be calculated, by integration using the Simpson method, of the equation:

$$Sh(t) = \overline{Pe}^{\frac{1}{3}} \int_0^1 \left(\frac{\partial C}{\partial y^*} \right)_{y^*=0} dx^* \quad (9)$$

The minimization of the difference between the numerical solution of the instantaneous Sherwood number $Sh_{num}(t_i^*)$ calculated via the convection diffusion equation by injection of an estimated wall shear stress $\overline{S}_{num}^*(t_i^*)$ and the experimental Sherwood number $Sh_{exp}(t^*)$ calculated via the limiting diffusion current $I_{exp}(t)$, allows the numerical determination of the wall shear stress [10]:

$$S_{exp}^*(t_i^*) = \overline{S}_{num}^*(t_i^*) + \frac{\left(Sh_{exp}^*(t_i^*) - \overline{Sh}_{num}^*(t_i^*) \right)}{\left(\frac{\partial \overline{Sh}_{num}^*(t_i^*)}{\partial S^*} \right)_{\overline{S}_{num}^*(t_i^*)}} \quad (10)$$

where $\left(\frac{\partial \overline{Sh}_{num}^*(t_i^*)}{\partial S^*} \right)_{\overline{S}_{num}^*(t_i^*)}$ is estimated numerically via the equation:

$$\left(\frac{\partial \overline{Sh}_{num}^*(t_i^*)}{\partial S^*} \right)_{\overline{S}_{num}^*(t_i^*)} = \frac{\left(\overline{Sh}_{num}^*(t_i^*, (1+\varepsilon)\overline{S}_{num}^*) - \overline{Sh}_{num}^*(t_i^*, (1-\varepsilon)\overline{S}_{num}^*) \right)}{2\varepsilon \overline{S}_{num}^*} \quad (11)$$

ε is chosen in the range $10^{-6} \leq \varepsilon \leq 10^{-3}$.

The new value of the wall shear stress obtained numerically $S_{num}^*(t_i^*)$ is injected again on the convection diffusion equation, in order to recalculate the new value of $Sh_{num}^*(t_i^*)$.

We should note that:

- In our study, we have chosen $\varepsilon = 10^{-4}$. This corresponds to an optimal value of the numerical derivate term $\left(\frac{\partial \overline{Sh}_{num}^*(t_i^*)}{\partial S^*} \right)_{\overline{S}_{num}^*(t_i^*)}$. This value permits to obtain a linear evolution between $Sh(t_i^*)$ and $S^*(t_i^*)$ according to Rehimy *et al.* [1].
- The estimated wall shear stress $\overline{S}_{num}^*(t_i^*)$ has to be well chosen for the proper operating of the method. In our study, Sobolik et al. [9] solution was used as an initial estimator $S_{num}^*(t^* = t_0^*) = S_{Sob}^*(t^* = t_0^*)$.
- A bad initialization of $S_{num}^*(t^* = t_0^*)$ needs a long calculation time for the resolution of the inverse problem in quasi-steady regime, which introduces a difference between the numerical solution and the experimental one at the beginning of the calculation.
- For high modulation amplitudes, the inverse method needs sufficiently smoothed signals to converge.

The inverse method was validated in previous works. It gives satisfactory results for reversing flows contrary to linear approaches of Lévêque [8] and Sobolik et al. [9].

The experimental mass transfer signals were smoothed (filtered) before using it to determine the wall shear rate because the different approaches are very sensitive to noise.

The temporal evolutions of wall shear rates, for relatively low modulation frequency $F = 100$ mHz, are presented respectively for modulation amplitude $\beta = 0.53$ and $\beta = 1.08$ on figure 13 (case A; $\beta = 0.53$) and Figure 14 (case B; $\beta = 1.08$).

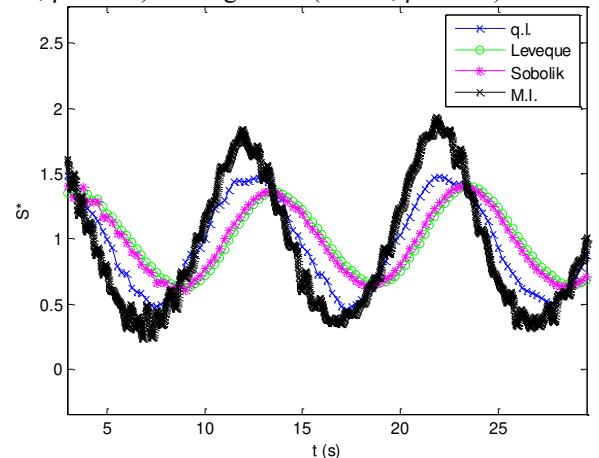


Figure 13. Evolution of dimensionless mass-transfer rate for $Ta_m=8$, $F=100$ mHz and $\beta=0.53$

The vortices manifest themselves by the presence of time-oscillations on wall shear rate evolution. For low modulation frequency ($F = 0.1$ Hz), comparing the results of modulation amplitudes $\beta = 0.53$ (i.e. nonstop advancing CT inner cylinder) to those of $\beta = 1.08$ (i.e. advancing - stop advancing CT inner cylinder), we proved that if the oscillation amplitude is “small” enough, the resulting time-dependent Taylor vortex rotates in a direction which depend on the direction of the azimuthal motion which drives it.

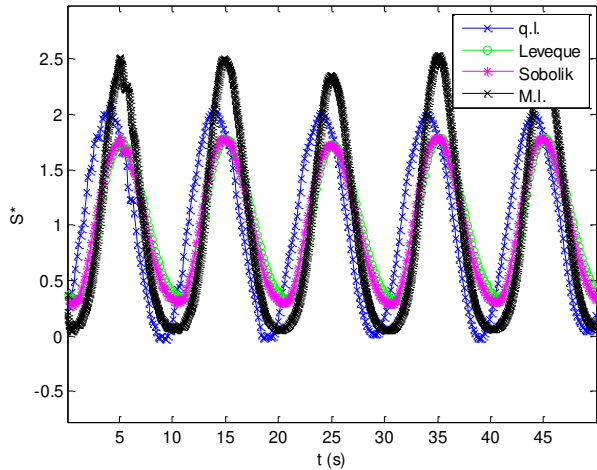


Figure 14. Evolution of dimensionless wall shear rate for $Ta_m=8$, $F=100$ mHz and $\beta=1.08$

6. MODULATION FREQUENCY EFFECT ON RTVF AND NRTVF

In this section, we analyze the modulation frequency effect on RTVF and NRTVF apparition by comparing the mass transfer and wall shear rates evolutions for relatively high oscillation frequencies ($F = 1000$ mHz and $F = 2000$ mHz) to those of the first section where the modulation frequency is equal to $F = 100$ mHz. The results presents the Taylor number, the mass transfer and the wall shear rate evolutions for different oscillation amplitudes; for example for the modulation amplitude $\beta = 1.08$ (figure 15 to 17); then for $\beta = 4.96$ (case C.2); $\beta = 9.73$ (case C.4) for $F = 1000$ mHz and $F = 2000$ mHz. This allows us to analyze also the effect of modulation amplitude for high modulation frequencies.

For a mean Taylor number equals to 8 and for relatively high modulation frequency ($F = 1000$ Hz), for a modulation amplitude $\beta = 1.08$, even if the inner cylinder stops i.e. the Taylor number is equal to zero in such moments (figure 16), the mass transfer rate remains positive (figure 17) and the wall shear rate (figure 18) is not equal to zero on the appropriate moment, thus the vortices do not disappear, contrarily, they continue to advance. The Taylor vortices direction does not change.

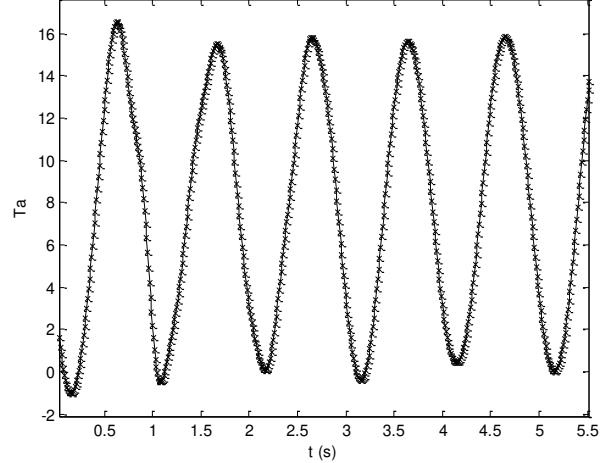


Figure 15. Evolution of the Taylor number for $Ta_m=8$, $F=1000$ mHz and $\beta=1.08$ (case B)

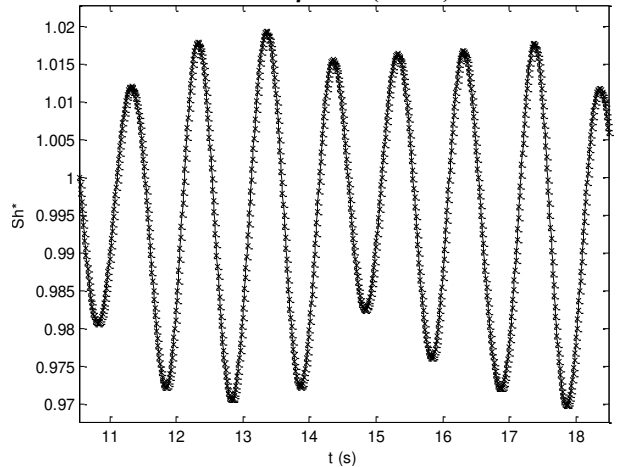


Figure 16. Evolution of dimensionless mass transfer rate for $Ta_m=8$, $F=1000$ mHz and $\beta=1.08$ (case B)

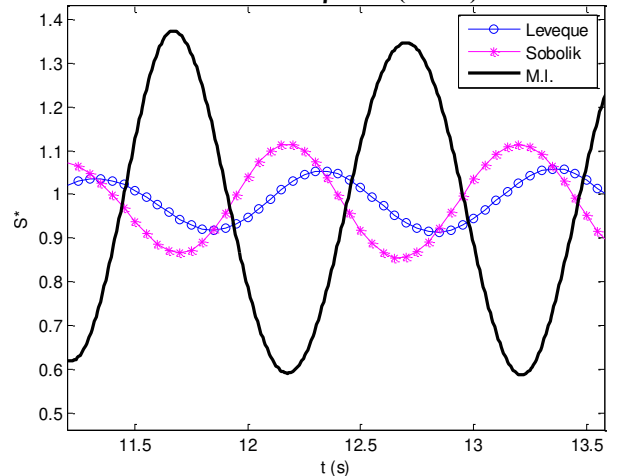


Figure 17. Evolution of dimensionless wall shear rate for $Ta_m=8$, $F=1000$ mHz and $\beta=1.08$ (case B)

The evolution of the Taylor number for $Ta_m = 8$, $F = 1000$ mHz, $\beta = 4.96$ (case C.1) is presented on figure 18. While the evolution of the mass transfer rate and the wall shear rate are respectively presented on figures 19 and 20. The inner cylinder

rotates anti-clockwise for the first part of the cycle; the vortices respond by rotating in the same direction of the cylinder motion. For the second part of the cycle, the inner cylinder rotates in the opposite direction, the vortices respond by changing their rotation direction. This corresponds to Reversing Taylor Vortex flow (RTVF).

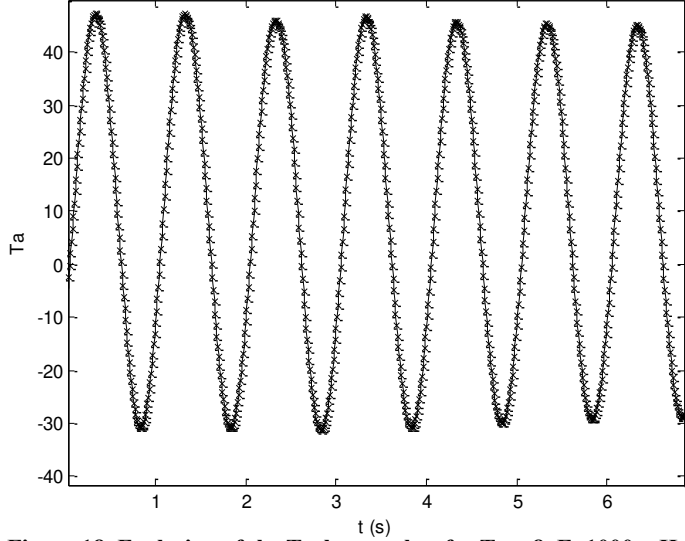


Figure 18. Evolution of the Taylor number for $Ta_m=8$, $F=1000$ mHz and $\beta=4.96$ (case C.1)

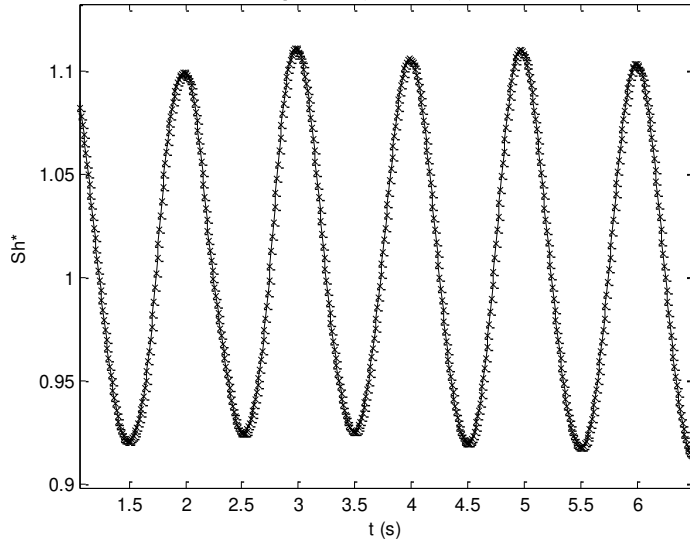


Figure 19. Evolution of dimensionless mass transfer rate for $Ta_m=8$, $F=1000$ mHz and $\beta=4.96$ (case C.1)

Comparing the results for $F = 0.1$ Hz, $F = 1$ Hz and $F = 2$ Hz, we demonstrated that for relatively high oscillation frequencies, the Taylor vortices direction change every half-cycle, i.e. presence of Reversing Taylor Vortex Flow (RTVF). There is apparition of Reversing Taylor Vortex Flow (RTVF) in which the rotation direction of the Taylor vortices is dependent on the inner cylinder rotation direction.

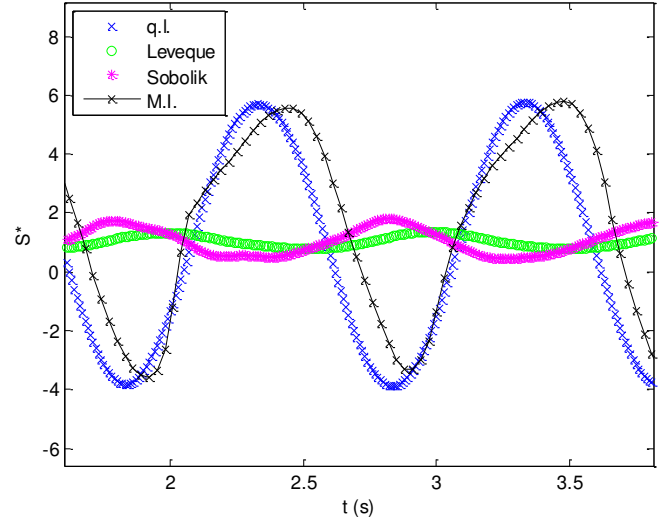


Figure 20. Evolution of dimensionless wall shear rate for $Ta_m=8$, $F=1000$ mHz, $\beta=4.96$ (case C.1)

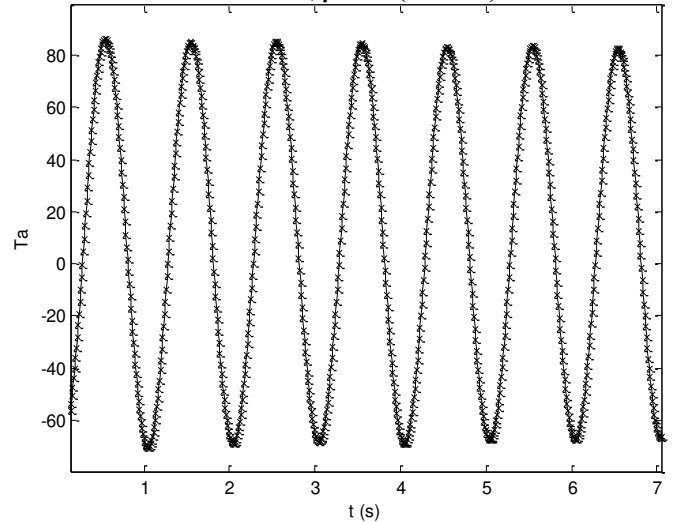


Figure 21. Evolution of Taylor number for $Ta_m=8$, $F=1000$ mHz and $\beta=9.73$ (case C.2)

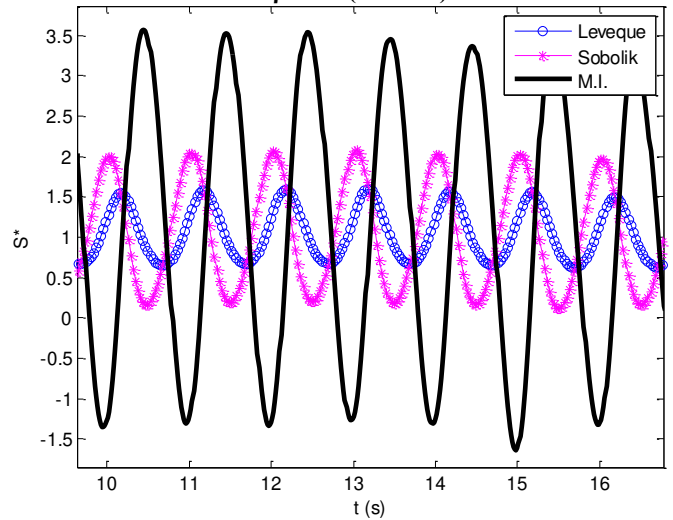


Figure 22. Evolution of dimensionless wall shear rate for $Ta_m=8$, $F=1000$ mHz and $\beta=9.73$ (case C.2)

According to the numerical study of Youd et al., [5] for Couette-Taylor system characterized by a radial ratio $\eta=R_{\text{int}}/R_{\text{out}}=0.75$, NRTVF takes place at sufficiently high modulation frequencies for which there is not enough time for the toroidal motion to change its direction. Thus, Taylor vortex always rotates in the same direction, despite the inner cylinder driving the flow in the opposite direction. However, in our experimental investigation for the study of Couette-Taylor system characterized by a radial ratio $\eta=R_{\text{int}}/R_{\text{out}}=0.97$; we proved experimentally that for frequencies modulation lesser than $F=2$ Hz and for modulation amplitude lesser than $\beta=9.73$; Taylor vortices follow the direction of the inner cylinder i.e. RTVF. The high amplitude accords to vortices sufficient time to follow the direction of the inner cylinder despite the relatively high frequency which seems to be not enough to have NRTVF.

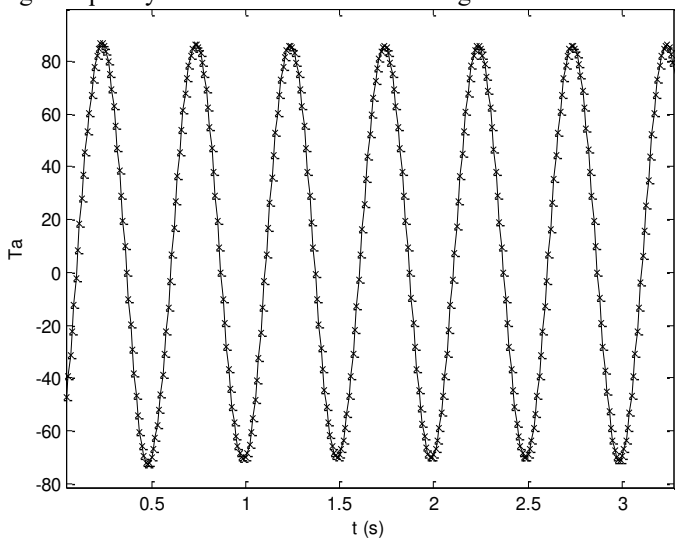


Figure 23. Evolution of the Taylor number for $Ta_m=8$, $F=2000$ mHz and $\beta=9.73$ (case 2)

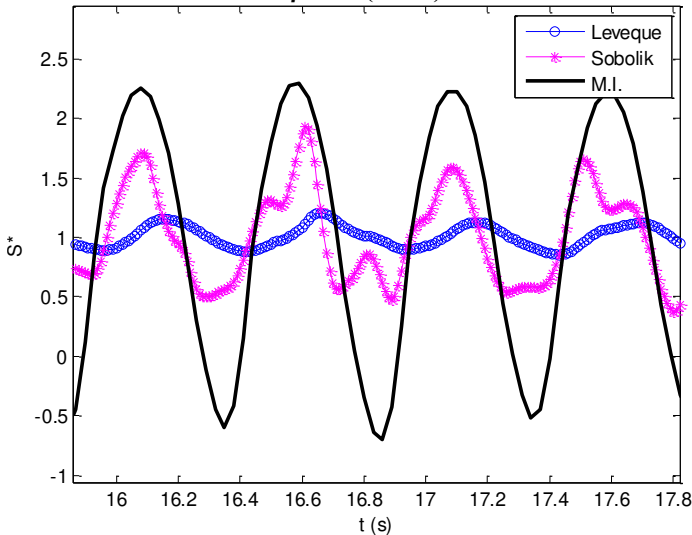


Figure 24. Evolution of dimensionless wall shear rate for $Ta_m=8$, $F=2000$ mHz and $\beta=9.73$ (case 2)

7. CONCLUSIONS

This paper presents an experimental investigation on oscillatory Couette-Taylor flows. Two experimental techniques were used: visualizations using Kalliroscope particles and the polarography technique known also as the Electro-Diffusion method. The vortices may manifest themselves by the presence of time-oscillations of mass transfer and wall shear rates, this generally corresponds to an instability apparition even for steady rotating cylinder. The wall shear rate was determined using three approaches: the “Lévêque solution” [8], Sobolik et al. [9] and the inverse method [10]. The results illustrate that if the modulation amplitude is large enough, it can destabilize circular Couette flow. The instantaneous and local mass transfer rates evolutions demonstrate the apparition and development of Taylor vortices which manifest themselves by the presence of oscillations having constant amplitudes for $\beta = 0.53$ and $\beta = 1.08$; and non constant amplitudes for sufficiently high amplitudes. For frequencies modulation lesser than $F = 2$ Hz and for modulation amplitude lesser than $\beta = 9.73$; Taylor vortices follow the direction of the inner cylinder i.e. Reversing Taylor Vortex Flow (RTVF). The high amplitude accord to vortices sufficient time to follow the direction of the inner cylinder despite the relatively high frequency which seems to be not enough to have Non-Reversing Taylor Vortex Flow (NRTVF).

ACKNOWLEDGMENTS

This work was supported by the laboratory GEPEA (University and École des Mines of Nantes) and the “Agence Nationale de la Recherche (ANR), France”, by the grant n° ANR-08-BLAN-0184-02. These supports are gratefully acknowledged.

REFERENCES

- [1] Youd A.J., Willis A.P., Barenghi C.F., Reversing and non-reversing modulated Taylor–Couette flow. *J. Fluid Mech.*, 487, 367–376, 2003.
- [2] Willis A. P., Barenghi C.F., Hydromagnetic Taylor-Couette flow: numerical formulation and comparison with experiment. *J. Fluid Mech.* 463, 361–375, 2002.
- [3] Barenghi C.F., Computations of transitions and Taylor vortices in temporally modulated Taylor–Couette flow. *J. Comput. Phys.*, 95, 175-194, 1991.
- [4] Jones C.A., Numerical methods for the transition to wavy Taylor vortices. *J. Comput. Phys.*, 61, 321-344, 1985.
- [5] Youd A.J., Willis A.P., Barenghi C.F., Non-reversing modulated Taylor-Couette flows, *Fluid Dynamics Research*, 36, 61–73, 2005.
- [6] Lopez J.M., Marques F., Modulated Taylor-Couette flow: Onset of spiral modes, *Theor. Comput. Fluid Dyn.*, 16, 59–68, 2002.
- [7] Carmi S., Tustaniwskyj J.I., Stability of modulated finite-gap cylindrical Couette flow: linear theory. *J. Fluid Mech.* 108, 19-42, 1981.

[8] Lévêque M.A., Les lois de transmission de la chaleur par convection. Ann. Mines, Vol. 13, 381-412, 1928.

[9] Sobolik V., Wein O., J. Cermak, Simultaneous measurement of film thickness and wall shear stress in wavy flow of non-

Newtonian liquids. Collection Czechoslovak Chem. Commun., Vol. 52, 913-928, 1987.

[10] Rehim F., Aloui F., Ben Nasrallah S., Doubriez L., Legrand J., Inverse method for electrochemical diagnostics of flows. Int. J. of Heat and Mass Transfer, 49, 1242- 1254, 2006.